INT. J. NUM. METH. HEAT FLUID FLOW, VOL. 3, 267–276 (1993)

EFFECT OF AN OBSTRUCTION ON NATURAL CONVECTION HEAT TRANSFER IN VERTICAL CHANNELS—A FINITE ELEMENT ANALYSIS

R. K. SAHOO, A. SARKAR* AND V. M. K. SASTRI

Department of Mechanical Engineering, Indian Institute of Technology, Madras 600 036, India

ABSTRACT

The effect of a rectangular obstruction of different sizes on natural convection heat transfer in the case of a vertical channel has been analysed for T boundary conditions on the walls. A comparison of the Nusselt number values with those for plane channel is presented. For smaller obstruction depths and for asymmetric heating, there is not much variation of the results from a case of channel with a baffle for asymmetric heating. For large obstruction depths, the flow conditions show a behaviour similar to that of a channel with a backward-facing step.

KEY WORDS Natural convection Vertical channels FE analysis

NOMENCLATURE

d	obstruction depth
D	non-dimensional obstruction depth
F	non-dimensional adjusted inlet velocity in y direction
g	acceleration due to gravity
Gr_s	Grashof number $\dfrac{s^3 g\beta(T_w - T_\infty)}{\nu^2}$
h	heat transfer coefficient
k	fluid thermal conductivity
l	plate height
l_g	position of obstruction
L	non-dimensional plate or channel height
L_g	non-dimensional obstruction depth position
$\overline{Nu}$	average Nusselt number on the hot wall
$\overline{Nu}_a$	average Nusselt number after the obstruction depth
$\overline{Nu}_b$	average Nusselt number before the obstruction depth
$\overline{Nu}_0$	average Nusselt number over the obstruction depth
Ob. 25	channel with a rectangular obstruction depth size 0.25
Ob. 50	channel with a rectangular obstruction depth size 0.50
Ob. 100	channel with a rectangular obstruction depth size 1.00
p	pressure
p_α	ambient pressure
P	non-dimensional pressure, $(p - p_\alpha)/\rho u_0^2$
Pr	Prandtl number, ν/α
Ra_s	Rayleigh number, $Pr \cdot Gr_s$

* Department of Mechanical Engineering, Jadavpur University, Calcutta 700032, India

0961–5539/93/030267–10$2.00

Received April 1992
Revised September 1992

Ra^* modified Rayleigh number, Ra_s/L
s plate spacing
T fluid temperature
T_w hot wall temperature
T_α inlet fluid temperature
T_c cold wall temperature
u, v x, y component velocities
u_0 characteristic velocity, $\sqrt{\beta g(T_\omega - T_\alpha)\cdot s}$
U, V non-dimensional x, y component velocities
w_1 obstruction depth
W_1 non-dimensional obstruction depth
x, y x, y coordinates
X, Y non-dimensional x and y coordinates

Greek symbols

α thermal diffusivity
β thermal expansion coefficient of fluid
θ non-dimensional temperature
θ_ω non-dimensional hot wall temperature
θ_c non-dimensional cold wal temperature
ν kinetic viscosity of fluid
ρ density of fluid

Subscript

0 non-dimensional cold wall temperature is 0

INTRODUCTION

Natural convection flow in vertical channels is of interest in a number of engineering applications. As far as the cooling of electronic equipment and avionic packages are concerned, natural convection heat transfer has an important role for its simplicity and reliability. The principal objective of thermal control of electronic components is to maintain the service temperature, typically between 85 and 100°C. Investigations reveal that, components operating 10°C beyond the above limits can have a reduced reliability of 50%. Hence, accurate thermal control is necessary.

Many diverse flow situations in vertical channels have been investigated theoretically (on the basis of boundary layer equations), as well as experimentally. Significant contributions to the analytical literature have been made by several investigators. Peterson and Ortega[1] reviewed the literature for free convection in vertical channels with different boundary conditions. However, in most of the practical situations, the geometrical configurations of the electronic components are very complex. The presence of protrusions like an obstruction or a baffle makes the governing equations for such problems elliptic and very little information is available for such geometries[2]. Recently a numerical investigation with elliptic equations by Naylor *et al.*[3] in the case of a vertical channel has pointed out the shortcomings of the boundary layer analysis. Further, Said and Krane[4] stressed the need of more analysis for such geometries. They carried out an analytical and experimental investigation of natural convection heat transfer in vertical channels with a semicircular obstruction and showed that there is a reduction in average Nusselt number by 5% at a Rayleigh number $= 10^4$ to 40% at a Rayleigh number $= 10$, for uniform wall temperature condition compared to an unobstructed channel.

The present study is concerned with a finite element analysis of free convection in a vertical channel with a rectangular obstruction on the hot wall, with symmetric as well as asymmetric heating for a Rayleigh number range of 10^2 to 10^4. The mass balance iterative scheme used in the case of a vertical channel[5] has been used here to determine velocity, temperature and average Nusselt number behaviour for different sizes of the obstruction at the middle of the channel. The results are compared with the existing solutions for a parallel plate channel configuration[5].

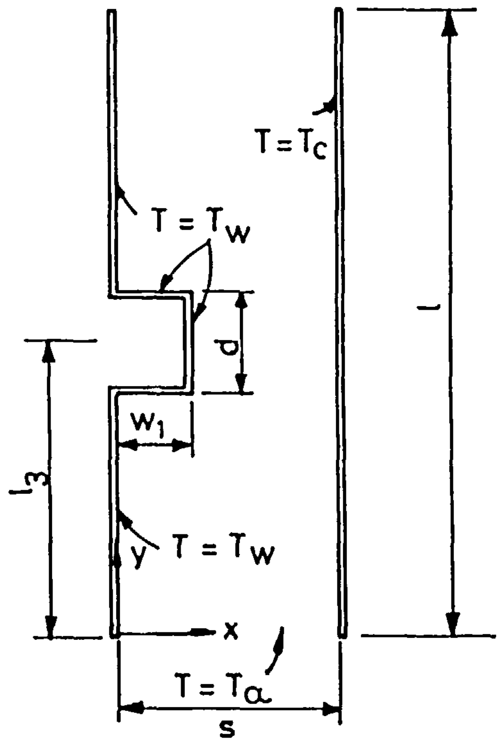

Figure 1 Physical model considered for analysis

GOVERNING EQUATIONS AND MATHEMATICAL FORMULATION

The physical model is as shown in *Figure 1.* For the analysis, considering the flow to be laminar, two-dimensional, incompressible and Boussinesq approximations are valid for free convection, the governing equations in non-dimensional form can be written as:

$$\frac{\partial U}{\partial X}+\frac{\partial V}{\partial Y}=0 \tag{1}$$

$$U\frac{\partial U}{\partial X}+V\frac{\partial U}{\partial Y}=-\frac{\partial P}{\partial X}+\frac{1}{A}\left[\frac{\partial^2 U}{\partial X^2}+\frac{\partial^2 U}{\partial Y^2}\right] \tag{2}$$

$$U\frac{\partial V}{\partial X}+V\frac{\partial V}{\partial Y}=-\frac{\partial P}{\partial Y}+\frac{1}{A}\left[\frac{\partial^2 V}{\partial X^2}+\frac{\partial^2 V}{\partial Y^2}\right]+\theta \tag{3}$$

$$U\frac{\partial \theta}{\partial X}+V\frac{\partial \theta}{\partial Y}=\frac{1}{A\cdot Pr}\left[\frac{\partial^2 \theta}{\partial X^2}+\frac{\partial^2 \theta}{\partial Y^2}\right] \tag{4}$$

where $A=\sqrt{Gr_s}=\sqrt{Ra_s/Pr}$.

The dimensionless parameters in the above equations are defined as:

$$U=\frac{u}{u_0} \qquad V=\frac{v}{u_0} \qquad X=\frac{x}{s} \qquad Y=\frac{y}{s}$$

$$\theta = \frac{T - T_\alpha}{T_w - T_\alpha}, \qquad P = \frac{P - P_\alpha}{\rho u_0^2} \quad \text{where } T_w \neq T_\alpha$$

Since for free convection there is no characteristic velocity, the following characteristic velocity is considered because of temperature difference in the flow:

$$u_0 = \text{characteristic velocity} = \sqrt{\beta \cdot g(T_\omega - T_\alpha)s}$$

$$Gr_s = \frac{s^3 g\beta(T_\omega - T_\alpha)}{v^2}$$

Boundary conditions

$$\left.\begin{array}{l} U = V = 0 \\ \theta = 1 \end{array}\right\} \begin{array}{l} \text{for } X = 0 \text{ and } 0 < Y < L_g - D/2 \text{ and for } L_g + D/2 < Y \leqslant L \\ \text{for } X = W_1 \text{ and } L_2 - D/2 < Y < L_g + D/2 \\ \text{for } X = W_1 \text{ and } Y = L_g - D/2 \text{ and } Y = L_g + D/2 \end{array}$$

$$\left.\begin{array}{l} U = V = 0 \\ \theta = \theta_c \end{array}\right\} \text{for } X = 1 \text{ and } 0 \leqslant Y \leqslant L$$

By applying Bernoulli's principle at the inlet and outlet and non-dimensionalizing,

$$\left.\begin{array}{l} P = -0.5F^2 \\ V = F \\ \theta = 0 \end{array}\right\} \text{for } 0 \leqslant X \leqslant 1 \text{ and } Y = 0$$

$$P = 0.0 \,\} \text{ for } 0 \leqslant X \leqslant 1 \text{ and } Y = L$$

where $W_1 = w_1/s$, $L_g = l_g/s$.

For the present problem the following cases are analysed:

$$\begin{array}{ll} L_g = 5.0, D = 1.0, W_1 = 0.5 & \\ L_g = 5.0, D = 0.5, W_1 = 0.5 & \text{with } L = 10, \theta_c = 0, 0.5, 1 \\ L_g = 5.0, D = 0.25, W_1 = 0.5 & \end{array}$$

Calculation of heat flux and Nusselt number on the hot wall are done as given below.

The average Nusselt number on hot wall is calculated considering the heat flux at the wall and wall to fluid temperature difference.

From energy balance,

$$Nu_l = h\frac{x}{k} \qquad \text{and} \qquad -K\frac{\partial T}{\partial X} = h(T_w - T_\alpha) \tag{5}$$

Now, for average Nusselt number from the above equation,

$$\overline{Nu} = \frac{1}{l}\int_0^l h\frac{x}{k}\,\mathrm{d}y \tag{6}$$

By non-dimensionalizing, for channel with rectangular obstruction, this can be written as,

$$\overline{Nu} = \frac{1}{L}\left[\int_0^{L_g - D/2}\left(-\frac{\partial\theta}{\partial X}\right)_{x=0}\mathrm{d}Y + (1 - W_i)\int_{L_g - D/2}^{L_g + D/2}\left(-\frac{\partial\theta}{\partial X}\right)_{x=i-W_i}\mathrm{d}Y + \int_{L_g + D/2}^{L}\left(-\frac{\partial\theta}{\partial X}\right)_{x=0}\mathrm{d}Y\right] \tag{7}$$

FINITE ELEMENT FORMULATION

For the present work, primitive variable formulation is adapted to solve the equations by finite element method. The geometry is discretized considering an eight-noded quadrilateral with four variables U, V, P and θ at the corner nodes and only U, V, and θ at the intermediate to avoid the spurious nodes of pressure rise[6]. So far as the method solution is concerned, the simultaneous approach based on Newton–Raphson method is employed. The simultaneous equations are solved by a frontal solver[7,8]. By Galerkin's formulation, the system of (1)–(4) can be written as:

$$\int M^{\mathrm{T}}\left[\frac{\partial U}{\partial X}+\frac{\partial V}{\partial Y}\right]\mathrm{d}s^{\langle\theta\rangle}=F^{\langle\theta\rangle} \qquad (8)$$

$$\int N^{\mathrm{T}}\left[\left(U\frac{\partial U}{\partial X}+V\frac{\partial U}{\partial Y}+\frac{\partial P}{\partial X}-\frac{1}{A}\left(\frac{\partial^2 U}{\partial X^2}+\frac{\partial^2 U}{\partial Y^2}\right)\right)\right]\mathrm{d}s^{\langle\theta\rangle}=F_2^{\langle\theta\rangle} \qquad (9)$$

$$\int N^{\mathrm{T}}\left[U\frac{\partial V}{\partial X}+V\frac{\partial V}{\partial Y}+\frac{\partial P}{\partial Y}-\frac{1}{A}\left(\frac{\partial^2 V}{\partial X^2}+\frac{\partial^2 V}{\partial Y^2}\right)-\theta\right]\mathrm{d}s^{\langle\theta\rangle}=F_g^{\langle\theta\rangle} \qquad (10)$$

$$\int N^{\mathrm{T}}\left[U\frac{\partial \theta}{\partial X}+V\frac{\partial \theta}{\partial Y}-\frac{1}{A\cdot Pr}\left(\frac{\partial^2 \theta}{\partial X^2}+\frac{\partial^2 \theta}{\partial Y^2}\right)\right]\mathrm{d}s^{\langle\theta\rangle}=F_4^{\langle\theta\rangle} \qquad (11)$$

For the solution, Newton–Raphson method is used having the iteration form as shown in (12). The right hand side indicates the residual matrix. The element stiffness matrix is based on left hand side gradients of (13), called Jacobian matrix. The iteration form can be written as:

$$\xi^{K+1}=\xi^{K}-[J]^{-1}R^{K} \qquad (12)$$

where K is the iteration count and R is residual vector given by:

$$R=[R_U^T R_P^T R_V^T R_\theta^T]$$

$$\xi=[U^T P^T V^T \theta^T]^T$$

$$J \text{ is the Jacobian matrix} = [J]=\frac{\partial R}{\partial \xi^T} \qquad (13)$$

SOLUTION PROCEDURE

Initially, the inlet velocity (non-dimensional) F is considered as 1 for the first iteration and, for the rest of the iterations a comparison is made between the average mass flow at inlet and outlet. Depending on that, the inlet uniform velocity factor is changed till the desired accuracy is obtained. It is found for higher Ra_s that it is better to start with the initial $F=1$, whereas for lower Ra_s, it is better to start with an F value something between 0.1 and 0.3 so that the convergence is faster. It is observed that for higher Ra_s it takes a maximum of 12 iterations to converge while for lower Ra_s the number of iterations goes to 20–25.

RESULTS AND DISCUSSION

The physical model considered can be converted to certain types of other problems by considering certain conditions as given below:

(1) For $D=0$ it is a case of plane channel problem.
(2) For very small D the problem is a case of channel with a baffle.
(3) For large value of D the results can be compared with a case of a channel with a backward-facing step.

Grid independence

The different grid distributions are considered for mesh sizes keeping the maximum total number of elements within 300 (because of computational limitations). Apart from uniform grid distributions, this study is carried out for different non-uniform grid-distributions with finer meshes nearer to the wall and coarser meshes towards the inner side. In addition to this, to take care of the reversed flow situations, fine meshes are also considered towards outlet.

Nusselt number and heat transfer rates

In order to analyse the heat transfer rates from the hot wall with obstruction the Nusselt number is calculated based on (7). However, to have a clear picture about it, three different Nusselt numbers $\overline{Nu}_b$, $\overline{Nu}_0$, $\overline{Nu}_a$ are determined in addition to $\overline{Nu}$, which are shown in *Figures 2* to *7*. The behaviour of $\overline{Nu}_b$ (*Figure 2*) is similar to $\overline{Nu}$ behaviour in the case of a plane channel problem[5]. A comparison of results with those for a case of a channel with a baffle shows that, up to $Ra^* = 200$, it is nearly equal with only a small deviation, whereas, for $Ra^* > 200$ the results for obstruction are more than that of channel with baffle in the case of symmetric heating. A similar behaviour is also found for $\theta_c = 0$ and 0.5 with a large difference in $\overline{Nu}$ for higher Ra_g and θ_c approaching zero. This is because of the contribution of $\overline{Nu}_0$ in the case of asymmetric heating compared to symmetric heating.

A comparison of $\overline{Nu}_b$, $\overline{Nu}_0$, $\overline{Nu}_a$ shows the following study. A study of Nu_l before the obstruction shows exactly a similar behaviour as in the case of a plane channel. The variation of $\overline{Nu}_b$ with Ra^* given in *Figure 2* gives a clear idea about this. It shows that, in all the cases, the heat transfer rate remains almost the same before the obstruction. A small discrepancy in the value is mostly because of different D values considered in the three different cases. An analysis of Nu_l on the obstruction vertical plate shows that it starts with a higher value, thus showing the development of thermal boundary layer. But it is not much effective because the small zone present in front of the obstruction makes the fluid to attain a higher temperature for which there is a drop in heat flux for larger obstruction sizes. In fact, for very large obstruction sizes the trend of results can be extrapolated which will show a similar behaviour as in case of a channel with a backward-facing-step[9].

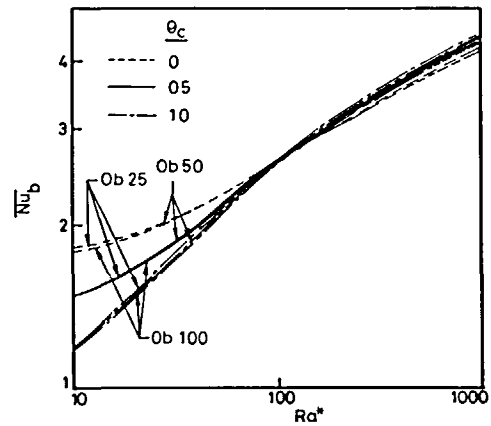

Figure 2 Variation of $\overline{Nu_l}$ with Ra^* for different obstruction sizes with various θ_c

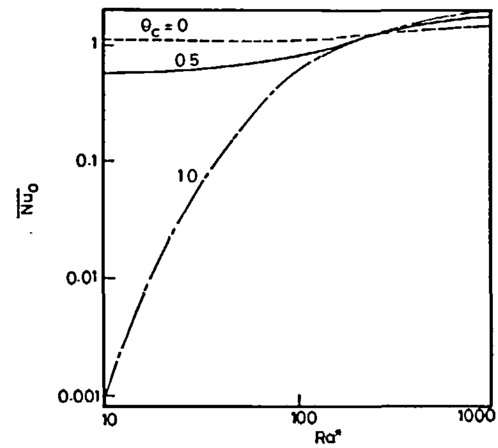

Figure 3 Variation of $\overline{Nu}_a$ with Ra^* for Ob. 100 with various θ_c

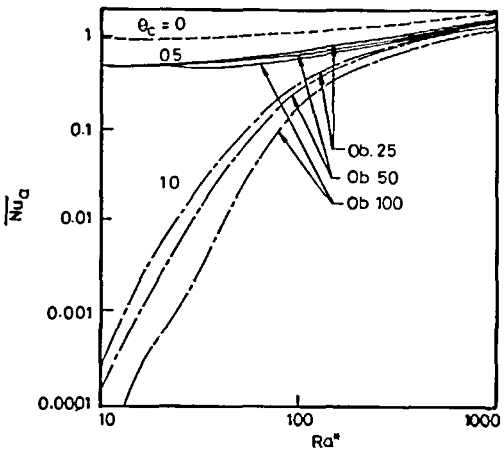

Figure 4 Variation of $\overline{Nu}_a$ with Ra^* for different obstruction sizes with various θ_c

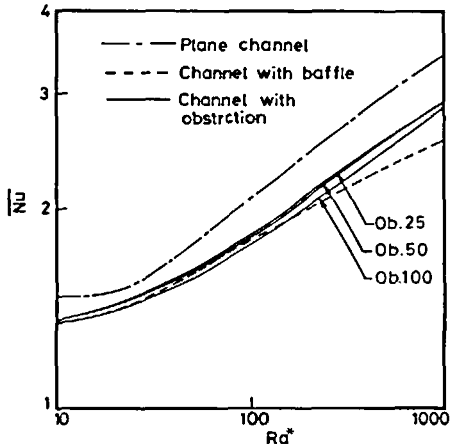

Figure 5 Variation of $\overline{Nu}$ with Ra^* for different obstruction sizes with $\theta_c = 0$

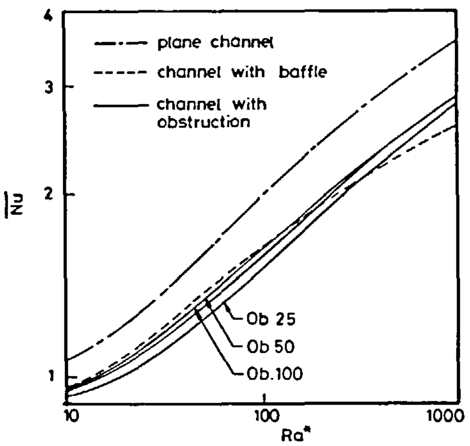

Figure 6 Variation of $\overline{Nu}$ with Ra^* for different obstruction sizes with $\theta_c = 0.5$

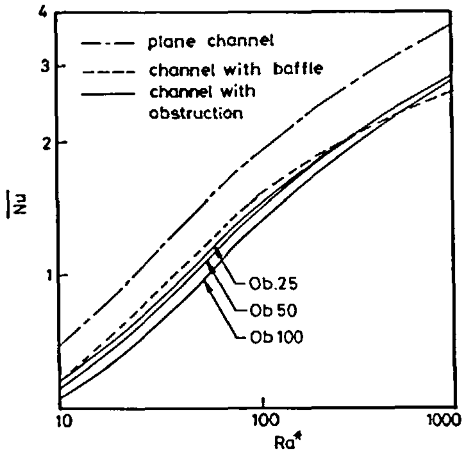

Figure 7 Variation of $\overline{Nu}$ with Ra^* for different obstruction sizes with $\theta_c = 1.0$

Temperature and velocity distribution

The isotherms shown in *Figures 8* to *10* show the following. For $\theta_c = 0$, the temperature variation shows a linear behaviour towards the exit. It also shows that, with increase in obstruction depth, the fluid attains maximum temperature within a short height.

The flow situation can be analysed by considering the absolute velocity distributions given in *Figures 11* to *13* for three different temperatures and three different sizes of the obstruction. It shows clearly that irrespective of θ_c value, no recirculation is found before the obstruction; thus the behaviour is similar to the case of plane channel problem. However, a zone of stagnation similar to the case of channel with a baffle is found here. As the zone of stagnation before the obstruction is very small compared to the zone of stagnation after the obstruction, the heat transfer rates are not much affected even if velocity is affected. For Ob. 25, in all the cases for

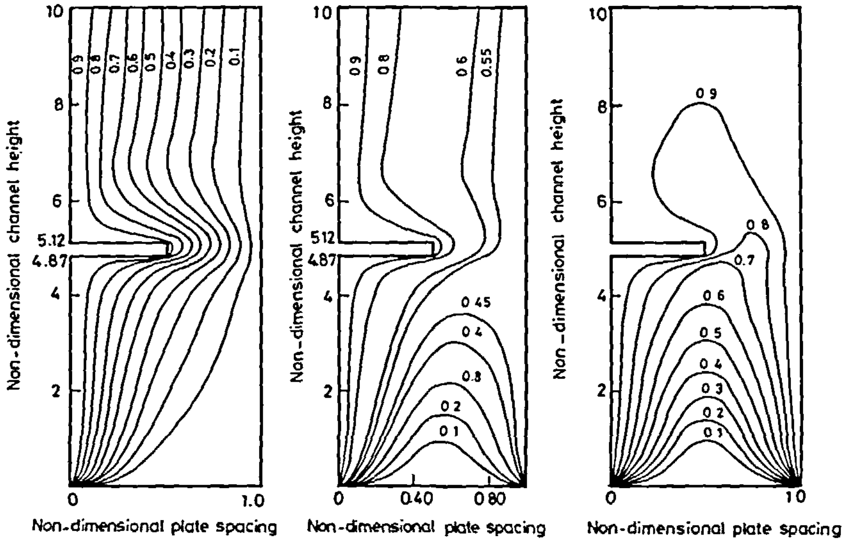

(a) ISOTHERMS FOR θ = 0 (b) ISOTHERMS FOR θ = 0.5 (c) ISOTHERMS FOR θ = 1.0

Figure 8

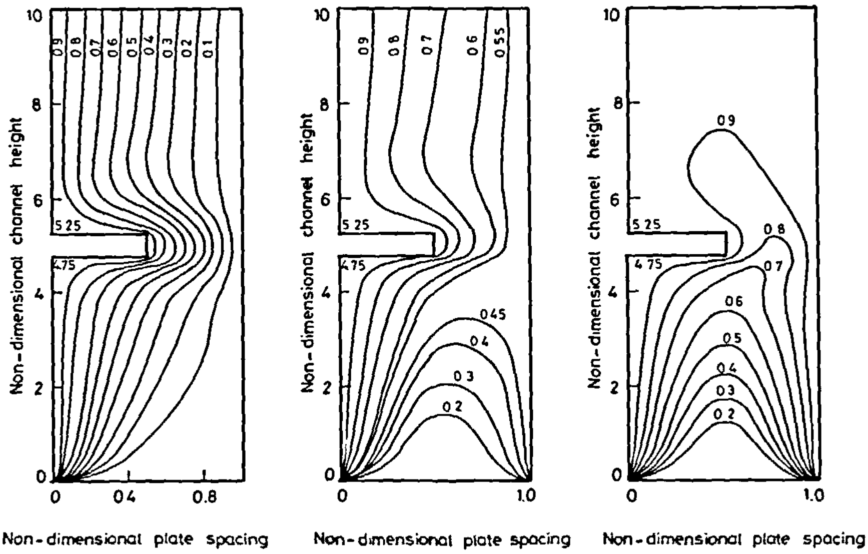

(a) ISOTHERMS FOR $\theta_c = 0$ (b) ISOTHERMS FOR $\theta_c = 0.5$ (c) ISOTHERMS FOR $\theta_c = 1.0$

Figure 9

the zone after obstruction, the recirculation is confined to $X = 0.25$. For $\theta_c = 0.0$, just after the obstruction for Ra_a less than 200, very feeble recirculation is found, but no recirculation is found near the cold wall. This proves that, even if the present problem is similar to a backward-facing step situation[9], no starved flow condition is found, because of the inflow of more fluid in the

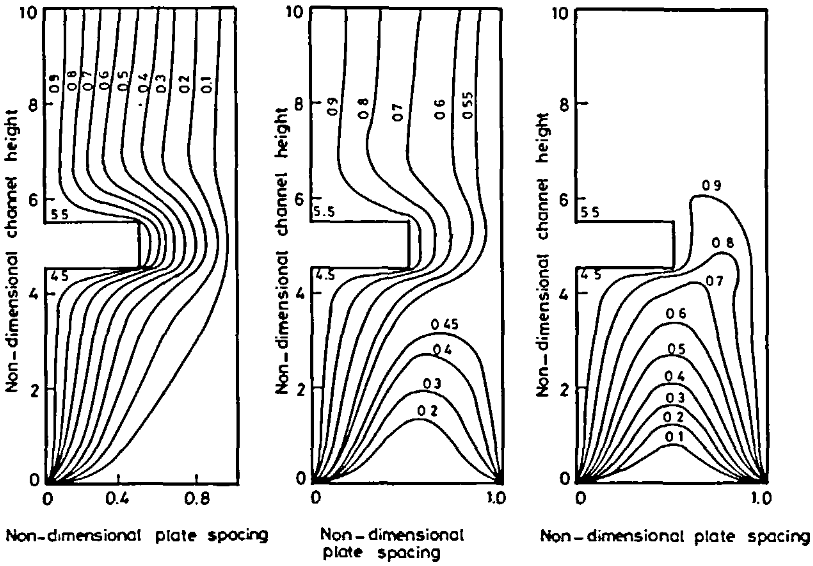

(a) ISOTHERMS FOR $\theta_c=0$ (b) ISOTHERMS FOR $\theta_c=0.5$ (c) ISOTHERMS FOR $\theta_c=1$

Figure 10

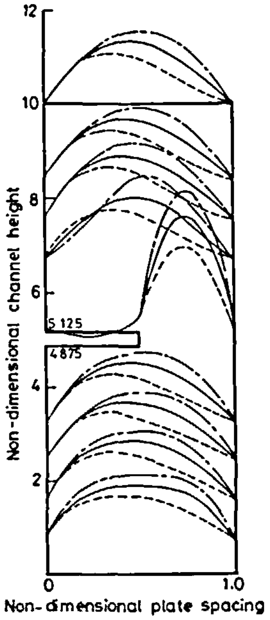

Figure 11 ABS velocities at different locations for Ob. 25

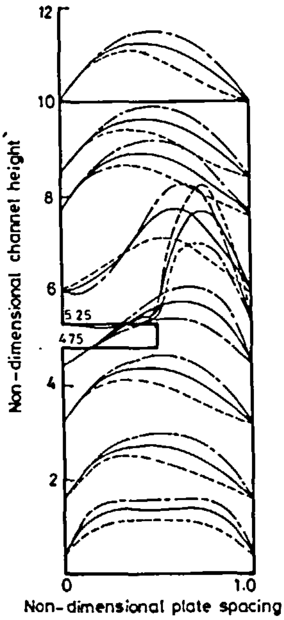

Figure 12 ABS velocities at different locations for Ob. 50

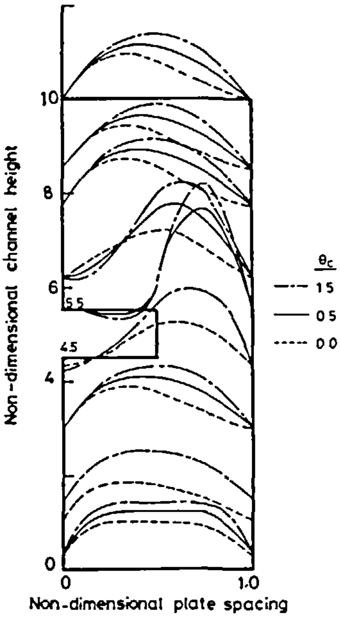

Figure 13 ABS velocities at different locations for Ob. 100

present case compared to the previous one. However, for Ra^* above 200 reversed flow is found near the cold wall for Y-value at which the recirculation near the hot wall ceases to exist. The reversed flow near the cold wall has a value of negative magnitude of velocity of the order of 25% of the magnitude of V_{max} found for that section. For $Ra^* = 10^3$ of Ob. 100_0 such a behaviour is more prominent. For $\theta_c = 0.5$ and 1, though the zone of recirculation over the obstruction becomes more and more prominent, no reversed flow is found. A comparison of the flow behaviour after the obstruction with either a case of channel with a baffle or backward-facing step indicates that the recirculation is mainly due to obstruction. Further, for large obstruction depths, the results can be compared with the case of a channel with a backward-facing step[9].

Correlation

The numerical results for average Nusselt number are correlated with obstruction depth besides Ra_g and θ_c as the parameters, having a correlation coefficient of 0.963. The correlation is:

$$\overline{Nu} = 0.152(Ra_g)^{0.258}(D)^{-0.090}(1 + \theta_c)^{-0.588} \tag{14}$$

for any θ_c value.

CONCLUSIONS

From the analysis of a vertical channel with a rectangular obstruction it is concluded that:

(1) a rectangular obstruction has no effect on the heat transfer rate before the obstruction, whereas, the heat transfer rate after the obstruction is very much affected, depending on the cold wall temperature and D;

(2) for small obstruction depth, the analysis can be considered as a case of channel with a baffle, while for large obstruction depth the results can be extrapolated for a channel with a backward-facing step;

(3) the zone of recirculation above the obstruction is due to the depth size, as no recirculation is observed for a channel with a baffle;

(4) for symmetric heating, the fluid attains maximum average temperature within a small height for low Rayleigh number or high obstruction depth.

REFERENCES

1 Peterson, G. P. and Ortega, A. Thermal control of electronic equipment and devices, *Adv. Heat Transfer*, **20**, (1990)

2 Aung, W. and Yener, Y. Research directions in natural convection, *Natural Convection Fundamentals and Applications*, (Ed. S. Kakac, W. Aung and R. Viskanta), Hemisphere, Washington DC (1985)

3 Naylor, D., Floryan, J. M. and Tarasuk, J. D. A numerical study of developing free convection between isothermal vertical plates, *J. Heat Transfer*, **113**, 620–626 (1991)

4 Said, S. A. M. and Krane, R. J. An analytical and experimental investigation of natural convection heat transfer in vertical channels with a single obstruction, *Int. J. Heat Mass Transfer*, **33**, 1121–1134 (1990)

5 Sahoo, R. K., Sarkar, A. and Sastri, V. M. K. Free convective flow in a vertical channel—a finite element study, *Proc. 7th Int. Conf. Num. Meth. Laminar Turb. Flow*, **VII**, Part 1, Pineridge Press, Swansea, pp. 155–165 (1991)

6 Olson, M. D. and Tuan, S. Y. Primitive variables *versus* stream function finite element solution of Navier–Stokes equations, *Finite Elements Fluids*, **3**, 73–87

7 Irons, B. M. A frontal solution program for finite element analysis, *Int. J. Num. Meth Eng.* **2**, 5–32 (1970)

8 Hood, P. Frontal solution program for unsymmetric matrices, *Int. J. Num. Meth. Eng.* **10**, 379–399 (1976)

9 Lin, J. T., Armaly, B. F. and Chen, T. S. Mixed convection in buoyancy-assisting, vertical channel backward-facing step flows, *Int. J. Heat Mass Transfer*, **33**, 2121–2132 (1990)